

Probing the electroweak symmetry breaking with Higgs production at the LHC

Ke-Pan Xie^{1,*} and Bin Yan^{2,†}

¹Center for Theoretical Physics, Department of Physics and Astronomy,
Seoul National University, 1 Gwanak-ro, Gwanak-gu, Seoul 08826, Korea

²Theoretical Division, Group T-2, MS B283, Los Alamos National Laboratory, P.O. Box 1663, Los Alamos, NM 87545, USA

The electroweak symmetry breaking (EWSB) mechanism is still an undecided question in particle physics. We propose to utilize the single top quark and Higgs associated production (th), Zh production via gluon fusion at the LHC to probe the couplings between the Higgs and the gauge bosons and further to test the EWSB. We demonstrate that the th and $gg \rightarrow Zh$ productions are sensitive to the relative sign of couplings ($ht\bar{t}$, hWW) and ($ht\bar{t}$, hZZ), respectively. We find that the relative sign between hWW and hZZ couplings could be fully determined after combining the present measurements from $gg \rightarrow h$, $t\bar{t}h$ and the th , Zh channels, as well as tZj and $Zt\bar{t}$ production at the 13 TeV LHC, and this conclusion is not sensitive to the possible new physics contribution induced by $Zt\bar{t}$ couplings in the $gg \rightarrow Zh$ production.

Introduction: Verifying the electroweak symmetry breaking (EWSB) mechanism is one of the major tasks of particle physics at the Large Hadron Collider (LHC) after the discovery of the Higgs-like boson [1, 2]. In the Standard Model (SM), the EWSB is triggered by the Brout-Englert-Higgs mechanism, in which the couplings of the Higgs to EW gauge bosons play a crucial role. Although their coupling strengths are predicted by the SM, many new physics (NP) models could have a different prediction. Observing a deviation in the gauge couplings from the SM prediction would shed light on various NP models and also the nature of EWSB.

Those gauge couplings are widely studied by both the theoretical [3–11] and experimental [12–16] groups within global analysis of Higgs data under the κ -scheme or the SM effective field theory (SMEFT) framework. Recently, both the ATLAS [14] and CMS [15, 16] collaborations show a strong constraint for the gauge couplings through a combined analysis of Higgs production and decay signal strengths within κ -scheme at the 13 TeV LHC, i.e. $\kappa_W = 1.10 \pm 0.08$, $\kappa_Z = 1.05 \pm 0.08$ (ATLAS) and $\kappa_W = 1.10 \pm 0.15$, $\kappa_Z = 0.99 \pm 0.11$ (CMS) with an assumption $\kappa_{W,Z} > 0$. Here $\kappa_{W,Z}$ are gauge coupling strength modifiers of Higgs to the W and Z bosons, i.e.

$$\mathcal{L}_{hVV} = \kappa_W g_{hWW}^{\text{SM}} h W_\mu^+ W^{-\mu} + \frac{\kappa_Z}{2} g_{hZZ}^{\text{SM}} h Z_\mu Z^\mu, \quad (1)$$

where $g_{hVV}^{\text{SM}} = 2m_V^2/v$ with $V = W, Z$ being the gauge couplings in the SM and $v = 246$ GeV. The modifier κ_V could be matched to the dimension-6 SMEFT operators after the EWSB [17–19], and should be a leading approximation of the SMEFT to parametrize the new physics in Higgs gauge couplings [20]. A global analysis to include Higgs, diboson and top quark measurements at the LHC in the framework of SMEFT with all possible

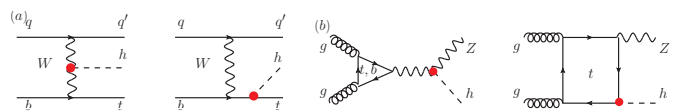


FIG. 1. Illustrative Feynman diagrams of th (a) and $gg \rightarrow Zh$ (b) production at the LHC. The red dots denote the effective couplings including both the SM and NP effects.

dimension-6 operators could be found in Ref. [21]. With higher luminosity data being accumulated, one expects the accuracy on κ_V could be further improved, e.g. the uncertainty will be reduced to 2% at the high-luminosity LHC (HL-LHC) [22], which operates at the $\sqrt{s} = 14$ TeV with an integrated luminosity of 3 ab^{-1} . However, the analysis based on the current Higgs signal strengths and the simulation of the future colliders can only constrain the magnitude of κ_V , while not the relative sign between κ_W and κ_Z . It has been shown in Ref. [23] that a negative ratio $\lambda_{WZ} \equiv \kappa_W/\kappa_Z$ is also possible in the NP models. It is crucial to determine both the sign and the magnitude of κ_V in order to further test the EWSB and search for the possible NP signals.

The sign of λ_{WZ} could be resolved through the Higgs golden decay channel $h \rightarrow ZZ^* \rightarrow 4\ell$ with $\ell = e, \mu$, due to the interference effects between the tree and loop level processes [24]. Alternatively, one can also use W^+W^-h [25] and vector bosons fusion production of Vh processes [26] at e^+e^- colliders to determine the sign of λ_{WZ} . In this work, we propose a novel method to pin down the sign of λ_{WZ} through the measurements of a Higgs boson with a single top quark (th) and $gg \rightarrow Zh$ production at the LHC; see Fig. 1. It is well known that the interference between the diagrams containing the $ht\bar{t}$ vertex and those containing the hWW vertex in th production is destructive when κ_t and κ_W have the same sign due to the unitarity [27, 28] (see Fig. 1(a)), where κ_t is the modifier of top quark Yukawa coupling,

$$\mathcal{L}_{htt} = -\frac{m_t}{v} \kappa_t h \bar{t} t. \quad (2)$$

* kpxie@snu.ac.kr

† Corresponding author: binyan@lanl.gov

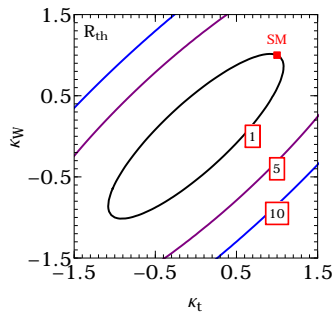


FIG. 2. The contours for $R_{th} = 1, 5$ and 10 in the plane of anomalous couplings κ_t and κ_W at the 13 TeV LHC.

We can therefore measure the sign of the $ht\bar{t}$ coupling respect to that of the hWW coupling through th production at the LHC [29–35]. Similarly the gluon-initiated Zh production is sensitive to the relative sign between $ht\bar{t}$ and hZZ couplings due to the cancelation between the box and triangle diagrams [32, 36–41]; see Fig. 1(b). Therefore, it would be promising to probe the sign of λ_{WZ} with the reference of $ht\bar{t}$ coupling through the measurements of th and $gg \rightarrow Zh$ production at the LHC. We will demonstrate in the following that combing the information of the $gg \rightarrow h$ production, $t\bar{t}h$ associated production and the two processes of we suggested, both the sign and magnitude of κ_V could be well constrained. **th production:** The th associated production can be classified into three channels: t -channel, s -channel and tW -channel. The higher order QCD and EW corrections under the SM and SMEFT have been discussed in Refs. [32, 42, 43]. The three channels share the same subprocess of $bW^\mu \rightarrow th$ and are related to each other by crossing symmetry. At high energy limit, the amplitude of $bW^\mu \rightarrow ht$ scattering will be dominated by the longitudinal polarized W boson and it could be written as,

$$M \sim \frac{1}{m_W^2} \bar{u}(t) \left[m_t (\kappa_t - \kappa_W) + \left(\frac{2m_W^2}{u} \kappa_W + \frac{m_t^2}{s} \kappa_t \right) \not{p}_W \right] P_L u(b). \quad (3)$$

Here s, t, u are the Mandelstam variables for describing the scattering of $bW \rightarrow th$. It clearly shows that there is a strong cancelation between $ht\bar{t}$ and hWW anomalous couplings at high energy. As a result, the cross section of th production can be significantly enhanced if the relative sign between $ht\bar{t}$ and hWW is reversed. In order to compare th cross section with non-standard $ht\bar{t}$ and hWW couplings to the SM prediction, we define a ratio R_{th} as,

$$R_{th} = \frac{\sigma(pp \rightarrow th)}{\sigma^{\text{SM}}(pp \rightarrow th)}. \quad (4)$$

Note that we include all three channels in R_{th} definition.

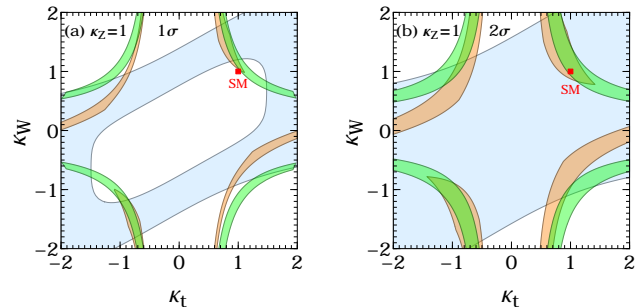


FIG. 3. Present constraints on the anomalous couplings κ_t and κ_W at the 13 TeV LHC. The light blue region comes from the th cross section measurement [45]. The orange and green bands correspond to the limits from $t\bar{t}h$ [45, 46] and $gg \rightarrow h \rightarrow WW^*$ [16], respectively.

Figure 2 displays the contours of $R_{th} = 1, 5$ and 10 in the plane of anomalous couplings κ_t and κ_W with CT14LO PDF [44]. The th production cross section could be enhanced up to one order of magnitude when $\kappa_t \kappa_W < 0$.

Recently, the th signal strength has been measured at the 13 TeV LHC by both the CMS (137 fb^{-1}) [45] and ATLAS (139 fb^{-1}) [46] collaborations, and the most stringent limit comes from the former, which is $\mu(th) = 5.7 \pm 2.7$ (stat) ± 3.0 (syst). In Fig. 3, we compare the precision on the determination of the Higgs anomalous couplings κ_t and κ_W via the measurements of inclusive cross section from th [45] (light blue), $t\bar{t}h$ [45, 46] (orange) and $gg \rightarrow h \rightarrow WW^*$ [16] (green), assuming $\kappa_Z = 1$. We summarize the signal strengths of Higgs production at the 13 TeV LHC in table I. The higher order QCD correction for th production processes have been included by a constant k -factor. A detail analysis of QCD correction for each anomalous couplings can be found in Ref. [32] and it shows that a constant k -factor should be a good approximation to parametrize the QCD effects. Furthermore, the scale and PDF uncertainties are around few percentage level at the NLO accuracy [32], and the results from 4-flavor and 5-flavor scheme provide fully consistent and similarly precise predictions for the total cross section and distributions [42]. Therefore, we expect the conclusion in this section should not strongly depend on those theoretical uncertainties. From Fig. 3, it is evident that the current measurements have favored same-sign κ_t and κ_W at around 2σ level, i.e. $\kappa_t \kappa_W > 0$ is required.

We remark that though we assume $\kappa_Z = 1$ in the analysis, the sign of $\kappa_t \kappa_W$ should not strongly dependent on this assumption since κ_Z will only change the Higgs total decay width, while not for the th scattering cross section. Moreover, the magnitude of κ_Z has been constrained severely at the LHC [14–16].

Zh production via gluon fusion: We consider the $ht\bar{t}$, hZZ and $Zt\bar{t}$ couplings to the $gg \rightarrow Zh$ production. The couplings of top quark to Z boson could be parametrized

| th [45] | $t\bar{t}h$ [45] | $t\bar{t}h$ [46] | ggF ($h \rightarrow WW^*$) [16] | ggF ($h \rightarrow ZZ^*$) [16] | - |
|------------------------|------------------------|------------------------|-----------------------------------|-----------------------------------|----------------|
| 5.7 ± 4.0 | $0.92_{-0.23}^{+0.26}$ | $1.43_{-0.34}^{+0.39}$ | $1.28_{-0.19}^{+0.20}$ | $0.98_{-0.11}^{+0.12}$ | - |
| Zh [47] | Zh [48] | Zh [49] | Zh [49] | Zh [50] | Zh [50] |
| $0.92_{-0.26}^{+0.28}$ | $1.08_{-0.23}^{+0.25}$ | $0.34_{-0.70}^{+0.75}$ | $0.28_{-0.83}^{+0.97}$ | 1.6 ± 0.89 | 1.2 ± 0.34 |

TABLE I. Signal strengths of Higgs production at the 13 TeV LHC.

generically with,

$$\mathcal{L}_{Ztt} = \frac{g_W}{2c_W} \bar{t} \gamma_\mu (\kappa_v^t v_t - \kappa_a^t a_t \gamma_5) t Z_\mu, \quad (5)$$

where g_W is the EW gauge coupling and c_W is the cosine of the weak mixing angle θ_W . The vector and axial-vector couplings of Z boson to top quark in the SM are $v_t = 1/2 - 4/3s_W^2$ and $a_t = 1/2$. The helicity amplitudes of $g(\lambda_1)g(\lambda_2) \rightarrow Z(\lambda_3)h$ with helicity $\lambda_i = \pm, 0$ for particle i have been calculated in Refs. [41, 51, 52]. It shows that the dominant amplitudes come from $(\pm, \pm, 0)$ helicity configurations and the results with $m_b = 0$ are [41],

$$M_{++0}^\Delta = 2 \frac{\sqrt{\lambda}}{m_Z} \sum_{t,b} \left[\kappa_a^q \kappa_Z \frac{a_q g_{hZZ}^{\text{SM}}}{m_Z^2} (F_\Delta(s, m_q^2) + 2) \right] N, \\ M_{++0}^\square = \frac{4m_t^2}{m_Z v \sqrt{\lambda}} \kappa_a^t \kappa_t a_t [F_{++}^0 + (t \leftrightarrow u)] N, \quad (6)$$

where

$$\lambda = s^2 + m_Z^4 + m_h^4 - 2(sm_Z^2 + m_Z^2 m_h^2 + m_h^2 s), \\ N = \frac{\alpha_s g_W}{32\pi c_W}. \quad (7)$$

The symbols Δ and \square denote the contributions from triangle and box diagrams, respectively (see Fig. 1(b)). The parameter $a_b = -1/2$ is the axial-vector coupling of Z boson to bottom quark and parameter $\kappa_a^b = 1$. Note that the helicity amplitudes $M_{--0}^{\Delta, \square}$ could be related to $M_{++0}^{\Delta, \square}$ by Bose symmetry [52]. The definition of the scalar functions F_Δ and F_{++}^0 in Eq. (6) could be found in Ref. [52]. We should note that only the axial-vector component (κ_a^t) of the $Zt\bar{t}$ couplings can contribute to the $gg \rightarrow Zh$ production due to the charge conjugation invariance [41].

At high energy limit, only the top quark contributes to the $gg \rightarrow Zh$ scattering and the total amplitude is,

$$M_{\pm, \pm, 0} \sim \frac{m_t^2}{m_Z^2} (\kappa_Z - \kappa_t) \log^2 \left(-\frac{s}{m_t^2} \right), \quad (8)$$

hence a strong cancellation occurs between the triangle and box diagrams in the SM where $\kappa_t = \kappa_Z = 1$. However, such relation could be violated in the NP models, so that the cancelation is spoiled and the Zh cross section would be enhanced.

Similar to R_{th} , we define a ratio R_{Zh} to compare the Zh scattering cross section with the SM prediction,

$$R_{Zh} = \frac{\sigma(gg \rightarrow Zh)}{\sigma^{\text{SM}}(gg \rightarrow Zh)}. \quad (9)$$

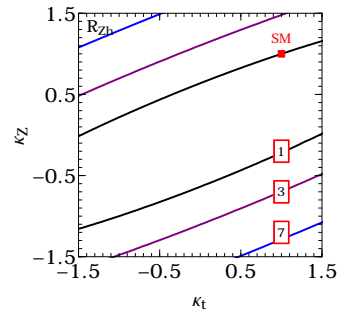
FIG. 4. The contours for $R_{Zh} = 1, 3$ and 7 in the plane of anomalous couplings κ_t and κ_Z at the 13 TeV LHC.

Figure 4 displays the contours of $R_{Zh} = 1, 3$ and 7 with $\kappa_a^t = 1$ and CT14LO PDF [44] in the plane of anomalous couplings κ_t and κ_Z . It shows that the cross section could be enhanced about few times compared to the SM prediction in the parameter space $\kappa_t \kappa_Z < 0$. On the other hand the $gg \rightarrow Zh$ production contributes $\sim 15\%$ to the total cross section of the $pp \rightarrow Zh$ process in the SM at the 13 TeV LHC. Therefore, few times enhancement of $gg \rightarrow Zh$ is a large enough deviation that can be detected at the LHC.

We note that both the inclusive cross section and transverse momentum distribution of Z boson in the $pp \rightarrow Zh$ production at the 13 TeV LHC have been measured by the ATLAS and CMS collaborations with integrated luminosities $79.8 \sim 139 \text{ fb}^{-1}$ [16, 47–50]. We show the limits from the present measurements to the plane of anomalous couplings κ_t and κ_Z with assumption $\kappa_W = \kappa_a^t = 1$ at 2σ level in Fig. 5. The light blue region denotes the constraint from the measurements of the $pp \rightarrow Zh$ production, in which both $q\bar{q}$ and gg initial states are considered. A constant k -factor has been used to mimic the higher order QCD correction effects for both $q\bar{q} \rightarrow Zh$ and $gg \rightarrow Zh$ production in the analysis, i.e. $k_{q\bar{q}} = 1.3$ and $k_{gg} = 2.7$ [53, 54]. It is worthwhile discussing how much our result will be influenced by the QCD corrections. The NNLO QCD corrections to the Zh production with the anomalous couplings have been discussed in Ref. [55] and it shows a constant k -factor should be a reasonable assumption in this work [55]. Furthermore, the scale uncertainty is around $1\% \sim 2\%$, as a result, the high order QCD effects should not alter the conclusion in this section. The orange and green bounds show the constraints imposed by the measurements of $t\bar{t}h$ [45, 46]

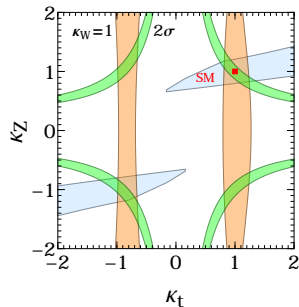


FIG. 5. Present constraints on the anomalous couplings κ_t and κ_Z with $\kappa_a^t = 1$ at the 13 TeV LHC. The light blue region comes from the inclusive cross section and transverse momentum distribution of Z boson in the $pp \rightarrow Zh$ production [16, 47–50]. The orange and green bands are corresponding to the limits from $t\bar{t}h$ [45, 46] and $gg \rightarrow h \rightarrow ZZ^*$ [16] production, respectively.

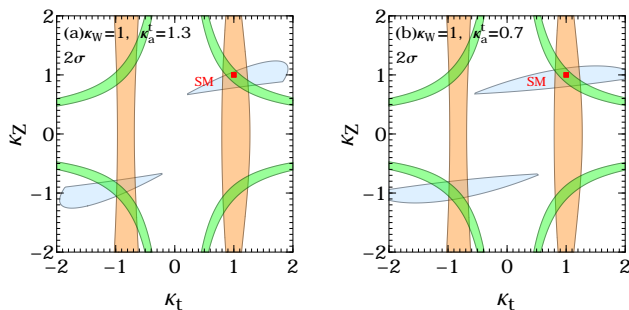


FIG. 6. Similar to Fig. 5, but for $\kappa_a^t = 1.3, 0.7$.

and $gg \rightarrow h \rightarrow ZZ^*$ production [16]; (see tabel I for the detail of the signal strengths.) It clearly shows that the current measurements of the Zh cross sections at the LHC has resolved the ambiguity of the relative sign between κ_t and κ_Z , i.e. $\kappa_t \kappa_Z > 0$ is allowed. Again, we emphasize that the sign $\kappa_t \kappa_Z$ should not be sensitive to the assumption of $\kappa_W = 1$ due to κ_W can not change the cross section of Zh scattering.

Next we consider the impact of the non-standard $Zt\bar{t}$

coupling to determine the relative sign between κ_t and κ_Z . The $Zt\bar{t}$ couplings have been well constrained by the measurements of tZj [56, 57] and $Zt\bar{t}$ [58, 59] productions at the 13 TeV LHC. The limits could be potentially improved after we combining the measurement from $gg \rightarrow ZZ$ production [60]. As a conservative estimation of the impact from the $Zt\bar{t}$ coupling, we choose two benchmark points of $\kappa_a^t = 0.7, 1.3$ in the analysis, and show the allowed parameter space of κ_t and κ_Z at 2σ level with above value of κ_a^t in Fig. 6. Although the value of κ_a^t will change the allowed parameter space of the κ_t and κ_Z from the Zh measurements, the relative sign between them is still fixed, i.e. $\kappa_t \kappa_Z > 0$.

Summary and discussion: Now equipped with the constraints for the Higgs couplings $ht\bar{t}$ and hWW (see Fig. 3), $ht\bar{t}$ and hZZ (see Fig. 5) at the 13 TeV LHC, we are ready to estimate the potential of pinning down the sign of λ_{WZ} through the global analysis of the $gg \rightarrow h$, $t\bar{t}h$ production and th , Zh scattering with present measurements. From the above discussion one sees that current data favors same sign for both the ($ht\bar{t}$, hWW) and ($ht\bar{t}$, hZZ) couplings, as a result, the $ht\bar{t}$ coupling could be a good reference to determine the relative sign between Higgs gauge couplings. In Fig. 7, we show the constraints on the plane of κ_Z and κ_W with $\kappa_t = 0.9, 1, 1.1$ and $\kappa_a^t = 1$ from the current measurements with (blue) and without Zh data (orange) at 2σ level. Although the Zh data itself can not improve the accuracy of the κ_V , the $\lambda_{WZ} < 0$ region could be excluded almost at 2σ level by Zh measurements, and this conclusion is not sensitive to possible new physics contribution induced by $Zt\bar{t}$ coupling in the $gg \rightarrow Zh$ production (see Fig. 6). At the HL-LHC, all the experimental measurements could be much improved compared to the current data, and as a result, we expect that the gauge couplings of Higgs to W and Z bosons could be well constrained and the nature of EWSB will surface at that time.

Acknowledgements: The authors thank Yandong Liu for helpful discussions and comments. B. Y. is supported by the U.S. Department of Energy, Office of Science, Office of Nuclear Physics, under Contract DE-AC52-06NA25396, [under an Early Career Research Award (C. Lee),] and through the LANL/LDRD Program. K. P. X. is supported by the Grant Korea NRF-2019R1C1C1010050.

[1] G. Aad et al. (ATLAS), Phys. Lett. B **716**, 1 (2012), 1207.7214.
 [2] S. Chatrchyan et al. (CMS), Phys. Lett. B **716**, 30 (2012), 1207.7235.
 [3] C. Englert, A. Freitas, M. Mühlleitner, T. Plehn, M. Rauch, M. Spira, and K. Walz, J. Phys. G **41**, 113001 (2014), 1403.7191.
 [4] K. Cheung, J. S. Lee, and P.-Y. Tseng, Phys. Rev. D **90**, 095009 (2014), 1407.8236.
 [5] J. Bergstrom and S. Riad, Phys. Rev. D **91**, 075008

(2015), 1411.4876.
 [6] A. Falkowski, Pramana **87**, 39 (2016), 1505.00046.
 [7] N. Craig, J. Gu, Z. Liu, and K. Wang, JHEP **03**, 050 (2016), 1512.06877.
 [8] T. Corbett, O. J. P. Eboli, D. Goncalves, J. Gonzalez-Fraile, T. Plehn, and M. Rauch, JHEP **08**, 156 (2015), 1505.05516.
 [9] G. Durieux, C. Grojean, J. Gu, and K. Wang, JHEP **09**, 014 (2017), 1704.02333.
 [10] J. De Blas, G. Durieux, C. Grojean, J. Gu, and A. Paul,

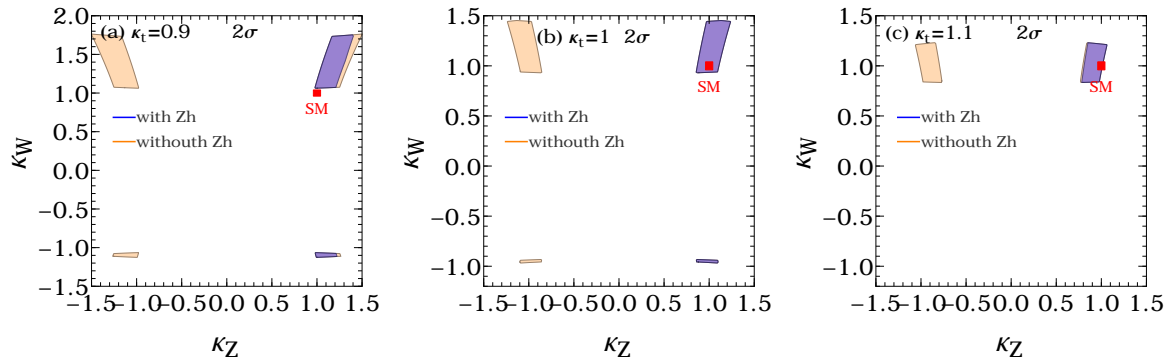


FIG. 7. Present constraints on the anomalous couplings κ_Z and κ_W at the 13 TeV LHC with $\kappa_t = 0.9, 1, 1.1$ and $\kappa_a^t = 1$. The blue region comes from the limits after we include all the data, while the orange band denotes the impact after we removing the Zh data (both the inclusive cross section and transverse momentum distribution of Z boson in $pp \rightarrow Zh$ production).

- JHEP **12**, 117 (2019), 1907.04311.
- [11] Q.-H. Cao, L.-X. Xu, B. Yan, and S.-H. Zhu, Phys. Lett. B **789**, 233 (2019), 1810.07661.
- [12] G. Aad et al. (ATLAS), Eur. Phys. J. C **76**, 6 (2016), 1507.04548.
- [13] V. Khachatryan et al. (CMS), Eur. Phys. J. C **75**, 212 (2015), 1412.8662.
- [14] G. Aad et al. (ATLAS), Phys. Rev. D **101**, 012002 (2020), 1909.02845.
- [15] A. M. Sirunyan et al. (CMS), Eur. Phys. J. C **79**, 421 (2019), 1809.10733.
- [16] Tech. Rep., CERN, Geneva (2020), URL <http://cds.cern.ch/record/2706103>.
- [17] W. Buchmuller and D. Wyler, Nucl. Phys. B **268**, 621 (1986).
- [18] G. Giudice, C. Grojean, A. Pomarol, and R. Rattazzi, JHEP **06**, 045 (2007), hep-ph/0703164.
- [19] B. Grzadkowski, M. Iskrzynski, M. Misiak, and J. Rosiek, JHEP **10**, 085 (2010), 1008.4884.
- [20] C. Arzt, M. B. Einhorn, and J. Wudka, Nucl. Phys. B **433**, 41 (1995), hep-ph/9405214.
- [21] J. J. Ethier, G. Magni, F. Maltoni, L. Mantani, E. R. Nocera, J. Rojo, E. Slade, E. Vryonidou, and C. Zhang (2021), 2105.00006.
- [22] Tech. Rep., CERN, Geneva (2018), URL <https://cds.cern.ch/record/2652762>.
- [23] I. Low and J. Lykken, JHEP **10**, 053 (2010), 1005.0872.
- [24] Y. Chen, J. Lykken, M. Spiropulu, D. Stolarski, and R. Vega-Morales, Phys. Rev. Lett. **117**, 241801 (2016), 1608.02159.
- [25] C.-W. Chiang, X.-G. He, and G. Li, JHEP **08**, 126 (2018), 1805.01689.
- [26] D. Stolarski and Y. Wu, Phys. Rev. D **102**, 033006 (2020), 2006.09374.
- [27] W. J. Stirling and D. J. Summers, Phys. Lett. B **283**, 411 (1992).
- [28] G. Bordes and B. van Eijk, Phys. Lett. B **299**, 315 (1993).
- [29] M. Farina, C. Grojean, F. Maltoni, E. Salvioni, and A. Thamm, JHEP **05**, 022 (2013), 1211.3736.
- [30] A. Kobakhidze, L. Wu, and J. Yue, JHEP **10**, 100 (2014), 1406.1961.
- [31] S. D. Rindani, P. Sharma, and A. Shivaji, Phys. Lett. B **761**, 25 (2016), 1605.03806.
- [32] C. Degrande, F. Maltoni, K. Mimasu, E. Vryonidou, and C. Zhang, JHEP **10**, 005 (2018), 1804.07773.
- [33] V. Barger, K. Hagiwara, and Y.-J. Zheng, Phys. Rev. D **99**, 031701 (2019), 1807.00281.
- [34] V. Barger, K. Hagiwara, and Y.-J. Zheng, JHEP **09**, 101 (2020), 1912.11795.
- [35] F. Maltoni, L. Mantani, and K. Mimasu, JHEP **10**, 004 (2019), 1904.05637.
- [36] C. Englert, M. McCullough, and M. Spannowsky, Phys. Rev. D **89**, 013013 (2014), 1310.4828.
- [37] B. Hespel, F. Maltoni, and E. Vryonidou, JHEP **06**, 065 (2015), 1503.01656.
- [38] D. Goncalves, F. Krauss, S. Kuttimalai, and P. Maierhöfer, Phys. Rev. D **92**, 073006 (2015), 1509.01597.
- [39] R. V. Harlander, J. Klappert, C. Pandini, and A. Papaefstathiou, Eur. Phys. J. C **78**, 760 (2018), 1804.02299.
- [40] E. Vryonidou and C. Zhang, JHEP **08**, 036 (2018), 1804.09766.
- [41] B. Yan and C. P. Yuan (2021), 2101.06261.
- [42] F. Demartin, F. Maltoni, K. Mawatari, and M. Zaro, Eur. Phys. J. C **75**, 267 (2015), 1504.00611.
- [43] D. Pagani, I. Tsirikos, and E. Vryonidou, JHEP **08**, 082 (2020), 2006.10086.
- [44] S. Dulat, T.-J. Hou, J. Gao, M. Guzzi, J. Huston, P. Nadolsky, J. Pumplin, C. Schmidt, D. Stump, and C. P. Yuan, Phys. Rev. D **93**, 033006 (2016), 1506.07443.
- [45] A. M. Sirunyan et al. (CMS) (2020), 2011.03652.
- [46] G. Aad et al. (ATLAS), Phys. Rev. Lett. **125**, 061802 (2020), 2004.04545.
- [47] M. Aaboud et al. (ATLAS), Phys. Lett. B **786**, 59 (2018), 1808.08238.
- [48] G. Aad et al. (ATLAS), Eur. Phys. J. C **81**, 178 (2021), 2007.02873.
- [49] G. Aad et al. (ATLAS), Phys. Lett. B **816**, 136204 (2021), 2008.02508.
- [50] M. Aaboud et al. (ATLAS), JHEP **05**, 141 (2019), 1903.04618.
- [51] B. A. Kniehl, Phys. Rev. D **42**, 2253 (1990).
- [52] B. A. Kniehl and C. P. Palisoc, Phys. Rev. D **85**, 075027 (2012), 1112.1575.
- [53] D. de Florian et al. (LHC Higgs Cross Section Working Group), **2/2017** (2016), 1610.07922.

- [54] A. Hasselhuhn, T. Luthe, and M. Steinhauser, *JHEP* **01**, 073 (2017), 1611.05881.
- [55] W. Bizoń, F. Caola, K. Melnikov, and R. Röntsch (2021), 2106.06328.
- [56] G. Aad et al. (ATLAS), *JHEP* **07**, 124 (2020), 2002.07546.
- [57] A. M. Sirunyan et al. (CMS), *Phys. Rev. Lett.* **122**, 132003 (2019), 1812.05900.
- [58] A. M. Sirunyan et al. (CMS), *JHEP* **03**, 056 (2020), 1907.11270.
- [59] M. Aaboud et al. (ATLAS), *Phys. Rev. D* **99**, 072009 (2019), 1901.03584.
- [60] Q.-H. Cao, B. Yan, C. Yuan, and Y. Zhang, *Phys. Rev. D* **102**, 055010 (2020), 2004.02031.